

## Role of the Structure and Electronic Properties of $\text{Fe}_2\text{O}_3\text{--MoO}_3$ Catalyst on the Dehydration of Isopropyl Alcohol

Abdel-Aziz Ahmed SAID

Department of Chemistry, Faculty of Science, Assiut University, Assiut, Egypt

(Received April 2, 1992)

Molybdenum oxide catalysts doped or mixed with (1—50) mol%  $\text{Fe}^{3+}$  ions were prepared. The structure of the original samples and calcined at 400 °C were characterized using DTA, X-ray diffraction, and IR spectra. The measurements of the electrical conductivity of calcined samples with and without isopropyl alcohol revealed that the conductance increases on increasing the content of  $\text{Fe}^{3+}$  ions up to 50 mol%. The activation energies of charge carriers were determined in presence and absence of alcohol. The catalytic dehydration of isopropyl alcohol was carried out at 250 °C using flow system. The results obtained showed that the doped or mixed catalysts are active and selective towards propene formation. However, the catalyst containing 40 mol%  $\text{Fe}^{3+}$  ions exhibited the highest activity and selectivity. Correlations were attempted between the catalyst composition and their electronic and catalytic properties. Probable mechanism for the dehydration process is proposed in terms of surface active sites.

Molybdenum oxide catalysts as a pure or mixed with foreign cations play an important role in the oxidation reactions.<sup>1–7)</sup> It was observed that almost all good oxidation catalysts have sites associated with single valency changes of cation. Such redox sites are often considered highly active both as adsorption sites and in electron exchange.<sup>8,9)</sup>  $\text{Fe}_2\text{O}_3\text{--MoO}_3$  catalysts are most widely used for the oxidation of methanol to formaldehyde. Extensive studies were concerned to the formation of iron molybdate spinel structure which shows a good activity and selectivity towards methanol oxidation to formaldehyde.<sup>10–12)</sup> Bhattacharya et al.<sup>13)</sup> reported that, iron molybdate decomposes into  $\alpha\text{-Fe}_2\text{O}_3$  and  $\text{MoO}_3$  on heating above 330 °C while Alessandrini et al.<sup>14)</sup> suggested that, the spinel is stable on heating up to 800 °C. However, the surface sites responsible for the reactions on the catalyst surfaces must be influenced by the change in the catalyst structure. Therefore, this work was devoted to characterize the structure and the active sites of the solid products of  $\text{Fe}_2\text{O}_3\text{--MoO}_3$  system in the range of doping and mixing. The structure was characterized by DTA, IR, and X-ray diffraction. The active sites involved in the reaction, the catalytic decomposition of isopropyl alcohol was carried together with the electrical conductivity in situ has been used.

### Experimental

**Materials.** Reagent grade chemicals were used in this work. A known weight of ammonium molybdate,  $(\text{NH}_4)_6\text{Mo}_7\text{O}_{24}\cdot 4\text{H}_2\text{O}$  was impregnated with the appropriate amount of  $\text{Fe}(\text{NO}_3)_3\cdot 9\text{H}_2\text{O}$  solutions with vigorous stirring at room temperature. The impregnated solids were dried at 100 °C in an oven to constant weight then calcined in air at 400 °C for 4 h. The content of  $\text{Fe}^{3+}$  ions added was varied between 1 to 50 mol%.

**Apparatus and Techniques.** Differential thermal analysis (DTA) of pure ammonium molybdate (AM) and mixed with  $\text{Fe}^{3+}$  ions was carried out using a Shimadzu Computerized

Thermal Analysis System DT-40. The system includes programmes which process data from the thermal analyzer with the chromatopac C-R3A. The rate of heating was kept at 10 °C  $\text{min}^{-1}$  in presence of air flow (40  $\text{ml min}^{-1}$ ).  $\alpha$ -Alumina powder for DTA standard material was applied as a reference.

Infrared spectra (IR) of the solid products were recorded using Perkin-Elmer Model SP3-300 infrared spectrophotometer in the range 1200—200  $\text{cm}^{-1}$  and KBr disc technique.

X-Ray diffraction patterns were recorded using a Philips diffractometer (model PW 1010). The patterns were obtained with Ni filter and Cu radiation. The diffraction lines were matched with ASTM cards.<sup>15)</sup>

The electrical conductivity measurements were carried out using a conductivity cell described previously.<sup>16)</sup>

The catalytic activity was tested using the vapor-phase decomposition of isopropyl alcohol (IPA) in a conventional gas flow system at atmospheric pressure. The system comprised of two reactors, one of them was used without any catalyst (control reactor), which enabled a measurement of the blank conversion which was subtracted from that measured with flow reactor. A reaction gas mixture of IPA with air was introduced into the fixed bed flow reactor. The exit feed was analyzed by direct sampling of the gaseous products into a PYE Unicam gas chromatograph which included a column of 3 m length and 0.5 cm diameter filled with 20% PEG and maintained at 100 °C.

### Results and Discussion

**Differential Thermal Analysis.** Figure 1 represents the DTA curves of pure AM and mixed with 30, 40, and 50 mol%  $\text{Fe}^{3+}$  ions. Curve (a) of pure AM exhibits four endothermic peaks. The first peak maximized at 124 °C, indicating removal of four molecules of water of crystallization bound to AM molecules.<sup>17)</sup> The second one located at 204 °C corresponds to the formation of the intermediate,  $(\text{NH}_4)_2\text{O}_4\text{MoO}_3$  whereas the third peak maximized at 300 °C due to the decomposition of this intermediate into  $\text{MoO}_3$ .<sup>18)</sup> The fourth peak maximized at 780 °C attributed to the sublimation of  $\text{MoO}_3$

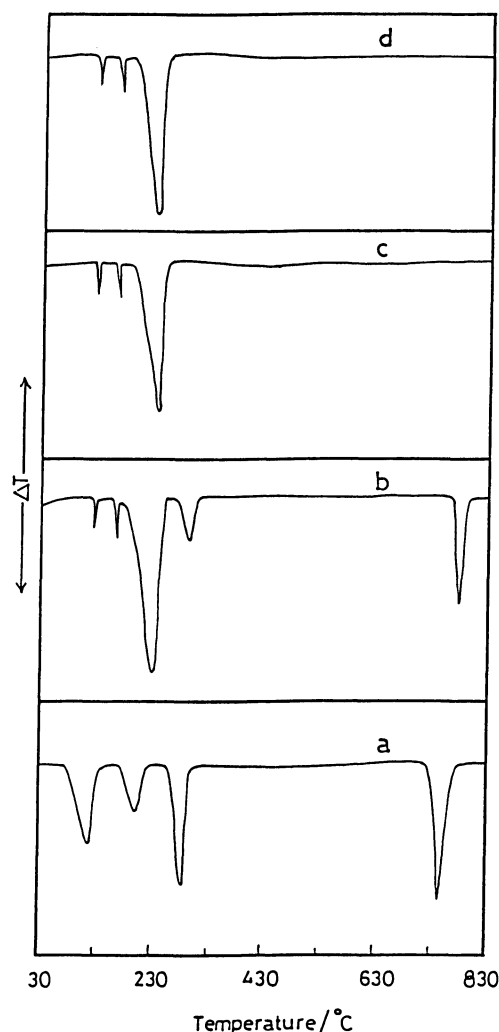


Fig. 1. DTA curves of pure AM (a) and mixed with  $\text{Fe}^{3+}$  ions, 30 mol% (b), 40 mol% (c), and 50 mol% (d).

solid.<sup>19)</sup> The addition of 30 mol%  $\text{Fe}^{3+}$  ions (curve b) shows that, the decomposition proceeds in three decomposition stages. The first endothermic peak located at 235 °C is probably due to the loss of water of crystallization of iron molybdate formed at this stage together with the formation of the intermediate,  $(\text{NH}_4)_2\text{O}_4\text{MoO}_3$ . The second endothermic peak maximized at 294 °C corresponds to the decomposition of the intermediate formed in the first stage into  $\text{MoO}_3$ . The third endothermic peak with the maximum at 776 °C is attributed to the sublimation of  $\text{MoO}_3$ . In fact, the decrease in the peak area corresponding to the decomposition of the intermediate indicates the participation of AM in the formation of iron molybdate. On increasing the ratios of  $\text{Fe}^{3+}$  ions, (curves c and d), the thermal decomposition proceeds in one stage on heating up to 800 °C. The endothermic peak maximized at 235 °C corresponds to the loss of water molecules, indicating that iron molybdate catalyst gets completely dehydrated above this temperature.<sup>13)</sup> Moreover, the absence of

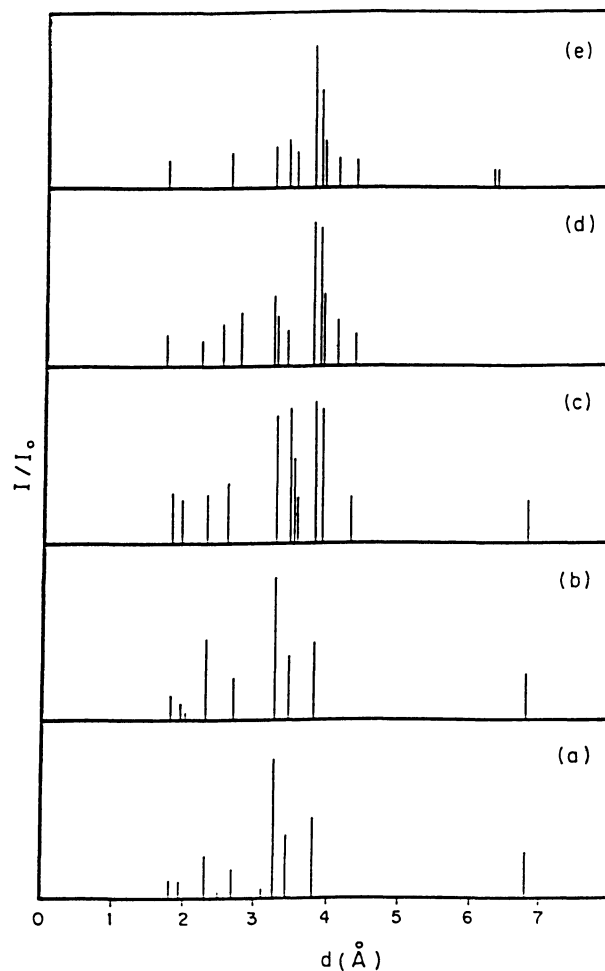


Fig. 2. X-Ray diffraction of pure  $\text{MoO}_3$  (a) and mixed with  $\text{Fe}^{3+}$  ions, 20 mol% (b), 30 mol% (c), 40 mol% (d), and 50 mol% (e) [The samples calcined at 400 °C for 4 h].

any peaks observed on heating up to 800 °C indicates the higher stability of the solid product and no excess  $\text{MoO}_3$  included. Bhattacharya et al.<sup>13)</sup> concluded that iron molybdate starts decomposing to amorphous iron-(III) oxide and molybdenum oxide above 330 °C. It is clear from the above results that iron molybdate spinel is stable on heating up to 800 °C which is in a good agreement with the results obtained by Alessandrini et al.<sup>14)</sup> Finally the two endothermic peaks maximized at 126 and 166 °C respectively, may be attributed to the decomposition of ammonium nitrate formed in the reaction mixture.<sup>20)</sup>

**X-Ray Diffraction.** Figure 2 shows the XRD patterns of pure  $\text{MoO}_3$  and mixed with 20, 30, 40, and 50 mol%  $\text{Fe}^{3+}$  ions preheated in air at 400 °C for 4 h. Curves (b and c) show the characteristic lines of  $\text{MoO}_3$  and iron molybdate,  $\text{Fe}_2(\text{MoO}_4)_3$ . The presence of  $\text{MoO}_3$  can be deduced from the occurrence of the lines at  $d=3.81$ , 3.49, 3.25 Å whereas the characteristic lines corresponding to the  $\text{Fe}_2(\text{MoO}_4)_3$  phase<sup>14)</sup> are located at  $d=4.07$ , 3.86, 3.46, and 2.96 Å. Curves (d and e) corre-

spond to the  $\text{MoO}_3$  mixed with 40 or 50 mol%  $\text{Fe}^{3+}$  ions indicating that the characteristic lines of  $\text{MoO}_3$  could not be detected. However, the detected lines confirm the formation of iron molybdate. These results support that the iron molybdate spinel can be formed without excess  $\text{MoO}_3$  in the presence of 40 mol%  $\text{Fe}^{3+}$  ions.

**IR Spectra.** IR spectra of  $\text{Fe}_2\text{O}_3$ - $\text{MoO}_3$  catalysts calcined at  $400^\circ\text{C}$  are shown in Fig 3. Curve (a) shows the absorption bands at  $990$  and  $870\text{ cm}^{-1}$  corresponding to the double bonded oxygen  $\text{Mo}=\text{O}$  and  $\text{Mo}-\text{O}-\text{Mo}$  lattice vibration modes.<sup>21,22</sup> Curve (b) shows that the addition of 30 mol%  $\text{Fe}^{3+}$  ions leads to a little lattice distortion of  $\text{MoO}_3$ . On addition of 40 or 50 mol%  $\text{Fe}^{3+}$  ions, curves (c and d) indicate the absence of the absorption bands corresponding to  $\text{MoO}_3$  and new bands appeared at  $930$ ,  $420$ , and  $340\text{ cm}^{-1}$ . These bands are attributed to the formation of iron molybdate.<sup>23</sup> The interest results are given in Fig. 4 for the IR spectra of the original samples of  $\text{MoO}_3$  mixed with 30, 40, or 50 mol%  $\text{Fe}^{3+}$  ions. It appears that, the bands corresponding to iron molybdate are located at the same position as that of the samples calcined at  $400^\circ\text{C}$ .

**Electrical Conductivity.** The electrical conductivity

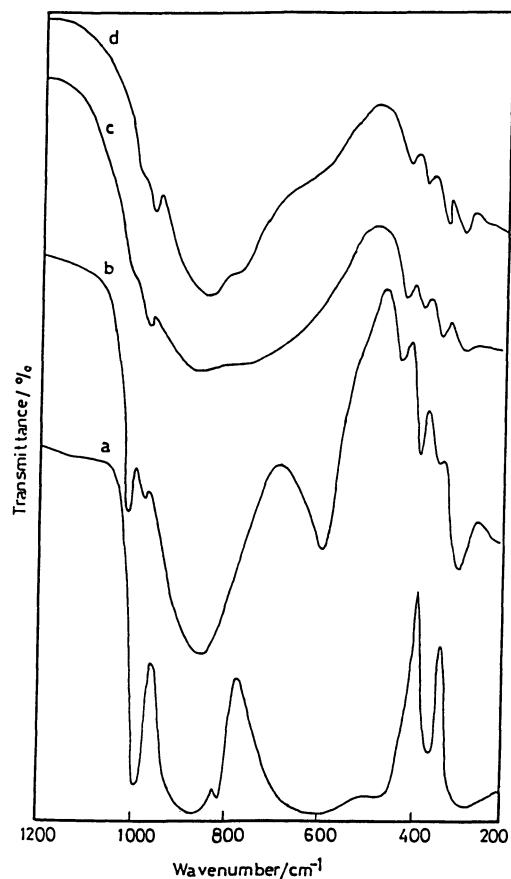


Fig. 3. IR Spectra of pure  $\text{MoO}_3$  (a) and mixed with  $\text{Fe}^{3+}$  ions, 30 mol% (b), 40 mol% (c), and 50 mol% (d) [The samples calcined at  $400^\circ\text{C}$  for 4 h].

measurements with and without IPA vapor atmosphere have been carried out at  $250^\circ\text{C}$  on all catalysts calcined at  $400^\circ\text{C}$ . The experimental conditions used were, 0.5 g catalyst and 1.7% reactant of IPA vapor in the gas feed. The flow rate of the carrier gas was  $300\text{ ml min}^{-1}$  (STP). The equilibrium conditions were obtained within 20–60 min depending on the catalyst composition and the reaction temperature. Figure 5 shows the variation of  $\log \sigma$  with the catalyst composition. Curve (a) appears that, without IPA (air only), the conductance increases on increasing the content of  $\text{Fe}^{3+}$  ions up to 50 mol%. This behavior indicates that, the presence

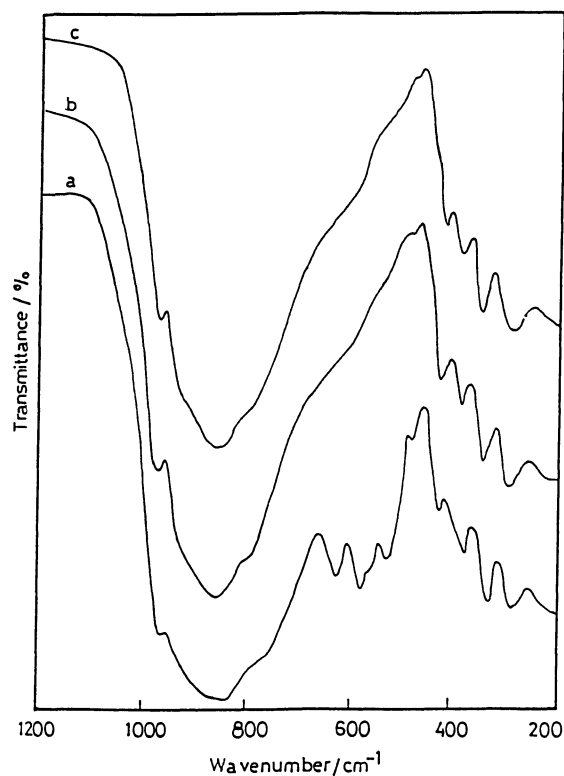


Fig. 4. IR Spectra of the original samples, of AM mixed with  $\text{Fe}^{3+}$  ions, 30 mol% (a), 40 mol% (b), and 50 mol% (c).

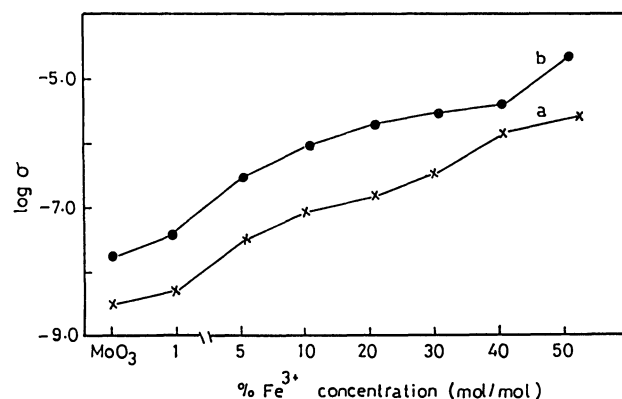
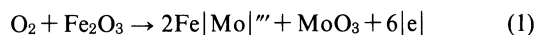


Fig. 5. The variation of  $\log \sigma$  with the % concentration of  $\text{Fe}^{3+}$  ions, without IPA (a) and with IPA (b).

of Fe<sub>2</sub>O<sub>3</sub> increases the charge carriers within MoO<sub>3</sub> lattice. This can be attributed to the creation of holes via Mo<sup>6+</sup> substituted Fe<sup>3+</sup> as the following equation:



where Fe|Mo|''' is a Fe<sup>3+</sup> cation substituting a lattice Mo<sup>6+</sup> and |e| is a hole. The creation of holes should enhance the electron mobility within MoO<sub>3</sub> lattice and consequently, increases its conductance. The effects of (IPA-air) mixture on the conductance values are shown in Fig. 5, curve (b). It appears that the conductance is higher than that of the conductance obtained in presence of air only. This indicates the increase of the charge carriers on the catalyst surface via the electron injected by IPA to the available accepting sites. The electronic theory of chemisorption on semiconducting materials postulates<sup>24)</sup> a close relation between the electronic properties of a catalyst and its catalytic activity. The width of the energy gap is important in controlling the number of molecules which can be chemisorbed in the course of a catalytic reaction and the nature of the chemical bond between the molecule and the surface. These factors control at the same time the activity and the mechanism of the catalytic reaction. Accordingly, the influence of the catalytic reaction temperature on the conductance with and without IPA was studied in the range (150–300 °C). The results indicated that the electronic exchange i.e. the conductance value increases on the increasing the reaction temperature. Plots of log  $\sigma$  against 1/*T* of pure MoO<sub>3</sub> and mixed with Fe<sup>3+</sup> ions can be fitted to an Arrhenius relationship,<sup>25)</sup>

$$\sigma = \sigma_0 \exp(-E_a/kT) \quad (2)$$

where  $E_a$  is the activation energy for conduction.

Table 1. The Electronic Exchange  $E_a$  in eV for Pure MoO<sub>3</sub> and Mixed with Fe<sup>3+</sup> Ions

Catalyst	$E_a$ (air)	$E_a$ (air+IPA)
Pure MoO <sub>3</sub>	0.92	0.81
20 mol% Fe <sup>3+</sup>	0.84	0.71
30 mol% Fe <sup>3+</sup>	0.65	0.53
40 mol% Fe <sup>3+</sup>	0.41	0.38
50 mol% Fe <sup>3+</sup>	0.66	0.56

Table 2. Variation of % Conversion, Yield and Selectivity of Pure MoO<sub>3</sub> and Mixed with Fe<sup>3+</sup> Ions at the Reaction Temperature of 250 °C

Fe <sup>3+</sup> / % (mol/mol)	Conversion	Yield / %		Selectivity / %	
	%	Propene	Acetone	Propene	Acetone
MoO <sub>3</sub>	80.6	73.5	5.0	91.2	6.2
1	85.5	78.5	3.8	91.8	4.4
5	89.5	82.3	2.5	92.0	2.8
10	91.2	85.1	1.5	93.3	1.6
20	92.5	87.5	1.4	94.6	1.5
30	94.1	89.5	1.4	95.1	1.5
40	98.5	97.0	1.4	98.5	1.4
50	88.5	82.0	2.6	92.6	2.9

Values of  $E_a$  obtained by the least squares fitting of the data are given in Table 1. From Table 1, it can be easily seen in absence of IPA that, the activation energies decrease on increasing Mo<sup>6+</sup> substituted Fe<sup>3+</sup> ions. The decrease in  $E_a$  values may be ascribed to the start of the formation of iron molybdate spinel structure and is consistent with the pairing probability for charge transfer proposed for hopping model. It was suggested that<sup>25–27)</sup> the charge carrier moves through the hopping polarons, which consists of a d-electron and its polarized region in the lattice. The observed minimum for composition of 40 mol% Fe<sup>3+</sup> ions, the optimum Fermi potential may be established.<sup>28)</sup> A further decrease in the activation energies in the presence of (IPA+air) is obtained. This behavior is probably due to the pinning of the Fermi energy to stabilize the density of electrons in the conduction band.<sup>28)</sup>

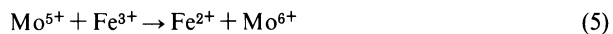
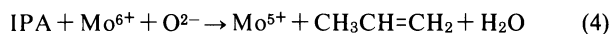
**Catalytic Activity Measurements.** The catalytic activity of various solids was determined using the same conditions used for the electrical conductivity. The reaction products were mainly propene with a minor yield of acetone. No products rather than propene and acetone were detected. The experimental results are tabulated in Table 2. Such results appear that the doped and mixed catalysts are active and selective towards propene formation compared with pure MoO<sub>3</sub> catalyst. Moreover, the catalyst which has the concentration of 40 mol% Fe<sup>3+</sup> ions possesses the highest activity and selectivity for the dehydration process. Furthermore, it is observed that, the dehydrogenation activity is little affected with the variation of the catalyst compositions. This means that the addition of Fe<sub>2</sub>O<sub>3</sub> only improves the sites responsible for the dehydration reaction. Therefore, we will consider only the dehydration reaction in the following discussion.

Based on the electron donating nature of the dehydration reaction of IPA,<sup>29)</sup> one can explain the higher activity and selectivity of Fe<sub>2</sub>O<sub>3</sub>-MoO<sub>3</sub> catalysts in terms of the coordination and electronic state of the active sites exposed in the surface planes which in turn is influenced by the electron availability at the surface. Although each plane is electrically neutral overall, many surface sites may not be all neutral but may have local positive or negative charges, and lowered coordinations. These sites, well seek to be neutralized by electron movement either by adsorption of an electron donor molecule, or by electron movement from the bulk of the solid.<sup>30)</sup> Accordingly, and based on the available data, one can suggest that, the increase in the dehydration reaction on addition of Fe<sub>2</sub>O<sub>3</sub> up to 10% mol may be explained on the basis of the doping effect of Fe<sup>3+</sup> ions, according to Eq. 1. The creation of holes together with Mo<sup>6+</sup> should enhance the chemisorption of IPA and consequently should increase the dehydration reaction.<sup>31,32)</sup> This suggestion is in accordance with the increase in log  $\sigma$  values in Fig. 5. The highest activity and selectivity of Fe<sub>2</sub>(MoO<sub>4</sub>)<sub>3</sub> spinel can be explained on the basis of its structure towards adsorption and activa-

tion of IPA. It was reported that<sup>33)</sup> the formation of iron molybdate is accompanied with the generation of molybdenum vacancies  $V_{Mo}^{6+}$  and oxygen vacancies  $V_{O}^{2-}$  as the following equation,



Moreover, it was suggested<sup>20)</sup> that the large density of oxygen vacancies in the active catalyst could be partially occupied with donors and provide as an impurity band that acts as a source and sink of electrons. From the results of activation energies, it can be suggested that, the decrease in its values should be facilitated by the electron exchange between IPA and the accepting sites on the catalyst surface during the reaction. In addition, Trifiro et al.<sup>34)</sup> concluded that, the whole catalyst (iron molybdate) participates in the reaction of methyl alcohol. This supports that iron cations can take place in the reaction pathways. Accordingly, based on the model proposed by earlier workers,<sup>35,36)</sup> the dehydration of IPA can occur on a pair of adjacent sites, viz.  $Mo^{6+}$  and  $O^{2-}$  as acidic and basic sites respectively. However, the dehydration reaction of IPA probably can be proceeded as follows,



It was reported that,<sup>37)</sup> the role of iron is to transfer water and oxygen between the catalyst surface and the gas phase. According to the above mechanism and based on the obtained results, it is clear that,  $Fe^{3+}$  ions hinder the reduction of  $Mo^{6+}$  cation which is consistent with the results reported.<sup>38,39)</sup> Thus, the presence of  $Mo^{6+}/Mo^{5+}$  and  $Fe^{3+}/Fe^{2+}$  as a redox cycles together with  $O^{2-}$  provides the active and selective surface sites. On the other hand the decrease in the activation energies during the reaction of IPA may be substantiated by the hopping mechanism of these cycles.

## References

- 1) A. M. El-Awad, E. A. Hassan, A. A. Said, and K. M. Abd El-Salaam, *Monatsh. Chem.*, **120**, 199 (1989).
- 2) J. Haber, E. Mielczavska, and W. Turek, *Z. Phys. Chem.*, **144**, 69 (1985).
- 3) G. I. Goldets, "Heterogeneous Catalytic Reduction Involving Molecular Oxygen," in "Studies in Surface Science and Catalysis," Elsevier, Amsterdam (1983), Vol. 15, Chap. XVI.
- 4) C. J. Materials, *ACS Symp. Ser.*, **178**, 239 (1982).
- 5) J. N. Allison and W. A. Godard, *J. Catal.*, **92**, 127 (1985).
- 6) P. Arnoldy, M.C. Franken, P. Scheffer, and J. A. Moulijn, *J. Catal.*, **96**, 38 (1985).
- 7) A. Satsumu, A. Hattori, K. Mitzutani, A. Furuta, A. Miyamoto, T. Hattori, and Y. Murakami, *J. Phys. Chem.*, **93**, 1484 (1989).
- 8) J. M. Peacock, A. J. Parker, P. G. Ashmore, and J. A. Hockey, *J. Catal.*, **15**, 373 (1969).
- 9) G. C. A. Schuit, *J. Less-Common Met.*, **36**, 329 (1974).
- 10) M. Carbucicchio and F. Trifiro, *J. Catal.*, **45**, 77 (1976).
- 11) C. J. Machiels and A. W. Sleight, *J. Catal.*, **76**, 238 (1982).
- 12) C. J. Machiels and A. W. Sleight, Proceedings of the 4th International Conf. on Chemistry and Uses of Molybdenum, Golden, Colorado, 1982, p. 411.
- 13) P. K. Bhattacharya, P. P. De, R. Jayannathan, and S. K. Bhattacharya, *Ind. Chem.*, **14**, 973 (1976).
- 14) G. Alessandrini, L. Cairati, P. Forzatti, P. L. Villa, and F. Trifir, *J. Less. Common Met.*, **54**, 373 (1977).
- 15) "Powder Diffraction File (Inorganic Compounds)," ed by W. F. McClune, JCPDS, PA (1978).
- 16) K. M. Abd El-Salaam and A. A. Said, *Surf. Technol.*, **17**, 199 (1982).
- 17) A. A. Ibrahim and G. A. El-Shobaky, *Thermochim. Acta*, **147**, 175 (1989).
- 18) W. J. Yong, *Thermochim. Acta*, **158**, 183 (1990).
- 19) "Handbook of Chemistry and Physics," The Chemical Rubber Publishing Company, Cleveand, OH (1961), p. 610.
- 20) K. J. Notz and P. A. Hass, *Thermochim. Acta*, **155**, 283 (1989).
- 21) F. Trifiro and I. Pasquon, *J. Catal.*, **12**, 412 (1968); P. C. H. Mitchell and F. Trifiro, *J. Chem. Soc. A*, **1970**, 3183.
- 22) J. R. Ferraro, "Low Frequency Vibration of Inorganic and Coordination Compound," Plenum Press, New York (1971).
- 23) P. L. Villa, A. Szabo, F. Trifiro, and M. Carbucicchio, *J. Catal.*, **47**, 122 (1977).
- 24) K. Haupe, *Adv. Catal.*, **7**, 213 (1955).
- 25) M. A. Dissanayake, O. A. Ileperuma, and P. A. Dharmasena, *J. Phys. Chem. Solids*, **50**, 352 (1989).
- 26) P. Pomonis and J. C. Vickerman, *J. Catal.*, **55**, 88 (1978).
- 27) D. Kumar, C. D. Parsad, and O. Parkash, *J. Phys. Chem. Solids*, **51**, 73 (1990).
- 28) K. Kimoto and S. R. Mirroson, *Z. Phys. Chem.*, **108**, 11 (1977).
- 29) A. A. Said, E. A. Hassan, E. M. El-Awad, and K. M. Abd El-Salaam, *Collect. Czech. Chem. Commun.*, **54**, 1508 (1989).
- 30) E. I. Odumah and J. C. Vickerman, *J. Catal.*, **62**, 195 (1980).
- 31) N. Giordano, M. Measa, A. Castellan, J. C. J. Bart, and V. Ragaini, *J. Catal.*, **50**, 342 (1977).
- 32) P. P. Vaishnava, P. A. Monatano, R. E. Tisher, and S. S. Pollack, *J. Catal.*, **78**, 454 (1984).
- 33) S. A. Halawy, Ph. D. Thesis, Assiut University, 1989.
- 34) F. Trifiro, S. Notarbartoloo, and I. Pasquon, *J. Catal.*, **22**, 324 (1971).
- 35) G. A. M. Hussein, N. Sheppard, M. I. Zakai, and R. B. Fahim, *J. Chem. Soc., Faraday Trans. 1*, **85**, 1723 (1989).
- 36) A. A. Said, *Collect. Czech. Chem. Commun.*, **50**, 2807 (1991).
- 37) F. Trifiro, V. DeVecchi, and I. Pasquon, *J. Catal.*, **15**, 8 (1969).
- 38) N. Pernicone, F. Lazzerin, G. Liberti, and G. Lanzavecchia, *J. Catal.*, **14**, 293 and 391 (1969).
- 39) J. Novakova, P. Jiru, and V. Zavadil, *J. Catal.*, **21**, 143 (1971).